BIOCHEMISTRY
including biophysical chemistry & molecular biology
Article

Biochemistry **2010,** *49,* 4349–4360 4349
DOI: 10.1021/bi100215b

Distinct Roles of Four Gelsolin-like Domains of *Caenorhabditis elegans* Gelsolin-like Protein-1 in Actin Filament Severing, Barbed End Capping, and Phosphoinositide Binding[†]

Zhongmei Liu, Tuula Klaavuniemi,[‡] and Shoichiro Ono*

Department of Pathology and Department of Cell Biology, Emory University, Atlanta, Georgia 30322 [‡]*Present address: University of Oulu, 90014 Oulu, Finland.*

Received February 11, 2010; Revised Manuscript Received April 12, 2010

ABSTRACT: *Caenorhabditis elegans* gelsolin-like protein-1 (GSNL-1) is a new member of the gelsolin family of actin regulatory proteins [Klaavuniemi, T., Yamashiro, S., and Ono, S. (2008) *J. Biol. Chem. 283*, 26071−26080]. It is an unconventional gelsolin-related protein with four gelsolin-like (G) domains (G1−G4), unlike typical gelsolin-related proteins with three or six G domains. GSNL-1 severs actin filaments and caps the barbed end in a calcium-dependent manner similar to that of gelsolin. In contrast, GSNL-1 has properties different from those of gelsolin in that it remains bound to F-actin and does not nucleate actin polymerization. To understand the mechanism by which GSNL-1 regulates actin dynamics, we investigated the domain−function relationship of GSNL-1 by analyzing activities of truncated forms of GSNL-1. G1 and the linker between G1 and G2 were sufficient for actin filament severing, whereas G1 and G2 were required for barbed end capping. The actin severing activity of GSNL-1 was inhibited by phosphatidylinositol 4,5-bisphosphate (PIP2), and a PIP2-sensitive domain was mapped to G1 and G2. At least two actin-binding sites were detected: a calcium-dependent G-actin-binding site in G1 and a calcium-independent G- and F-actin-binding site in G3 and G4. These results reveal both conserved and different utilization of G domains between *C. elegans* GSNL-1 and mammalian gelsolin for actin regulatory functions.

Actin filaments are relatively stable, and regulated disassembly of preexisting filaments is often a critical process for remodeling of the actin cytoskeleton in a number of dynamic cellular events (*1*). Severing of actin filaments is an effective way to initiate filament disassembly. Gelsolin-related proteins (*2*−*4*) and actin-depolymerizing factor (ADF)[1] and cofilin proteins (*5*−*7*) make up the two major classes of actin regulatory proteins that enhance actin filament turnover by severing and depolymerizing actin filaments. Gelsolin strongly severs actin filaments and caps the barbed ends in a calcium-dependent manner, while ADF/cofilin weakly severs actin filaments without capping filament ends in a calcium-independent manner. Thus, gelsolin and ADF/cofilin have different impacts on actin filament dynamics and distinct functions in regulating reorganization of the actin cytoskeleton.

Gelsolin has six repeats of homologous domains of 100−120 amino acids, which are designated as gelsolin-like (G) domains or segments (*2*−*4*). Despite the fact that the G domains of gelsolin have homologous sequences and three-dimensional structures, each G domain plays distinct roles in actin filament severing and capping. The most N-terminal G domain with a linker sequence is sufficient for actin filament severing (*8*) and capping (*9*). The first and fourth G domains bind to actin at a cleft between subdomains 1 and 3 (*10*−*13*), while the second G domain binds to actin subdomain 2 that remains exposed on the surface of F-actin (*12*, *14*, *15*). Calcium-free inactive gelsolin has a tightly packed globular conformation with a number of interdomain interactions (*16*). Calcium activation of gelsolin induces large domain movements by dissociating some of the interdomain interactions and exposing actin-binding sites (*12*, *13*, *17*). Thus, each G domain of gelsolin has either direct or indirect roles in the calcium-dependent actin regulatory activities.

G domains are found in many gelsolin-related proteins that have variable numbers of G domains ranging from two to six (*1*). However, roles of G domains of gelsolin-related proteins other than gelsolin in actin regulatory activities are poorly understood. We have recently reported that gelsolin-like protein-1 (GSNL-1) from *Caenorhabditis elegans* is a novel gelsolin-related protein with four G domains (*18*). GSNL-1 is similar to gelsolin in that it severs and caps actin filaments. However, unlike gelsolin, GSNL-1 remains bound to actin filaments and does not nucleate actin polymerization (*18*). Three N-terminal G domains of GSNL-1 are homologous to the equivalent regions of gelsolin, whereas the most C-terminal G domain of GSNL-1 is most closely related to the sixth G domain of gelsolin. Therefore, GSNL-1 lacks two G domains that are equivalent to the fourth and fifth G domains of gelsolin. These unique properties of GSNL-1 prompted us to dissect the functional domains of GSNL-1, as it can be a model for analyzing how multiple G domains coordinate to regulate actin filament dynamics. We found that G domains of GSNL-1

[†]This work was supported by grants from the National Institutes of Health (R01 AR48615) and the University Research Committee of Emory University to S.O.

*To whom correspondence should be addressed: Department of Pathology, Emory University, 615 Michael St., Whitehead Research Building, Room 105N, Atlanta, GA 30322. Telephone: (404) 727-3916. Fax: (404) 727-8538. E-mail: sono@emory.edu.

[1]Abbreviations: ADF, actin-depolymerizing factor; BSA, bovine serum albumin; C_c, critical concentration; CA, carbonic anhydrase; G domain, gelsolin-like domain; GSNL-1, gelsolin-like protein-1; GST, glutathione *S*-transferase; PIP2, phosphatidylinositol 4,5-bisphosphate.

Published on Web 04/14/2010

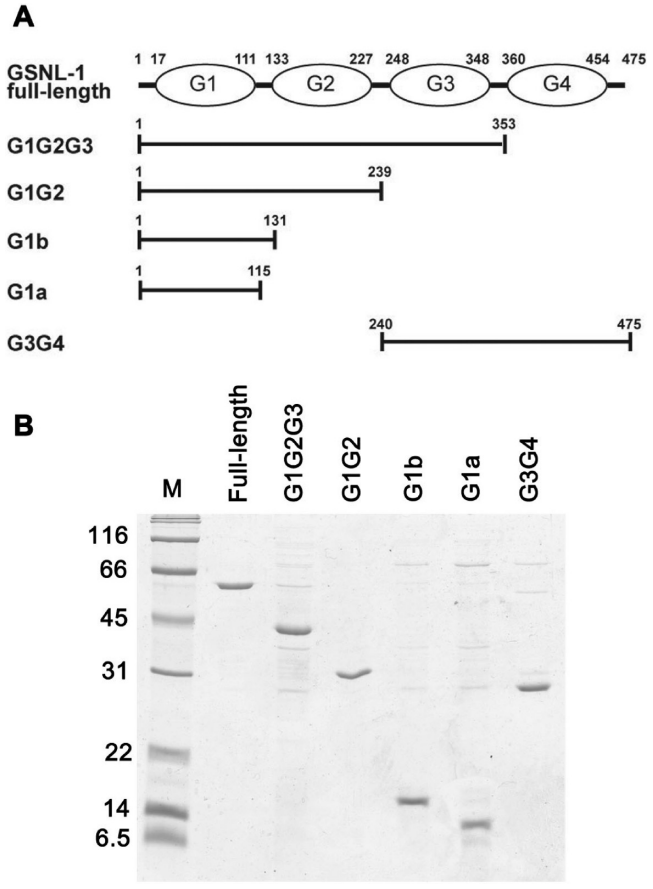

FIGURE 1: Expression and purification of GSNL-1 variants. (A) Schematic representation of the domain structure of full-length GSNL-1 (top). G domains are designated as G1−G4. Positions of N- and C-termini of each domain are shown at the top. Positions of amino acid sequences of each GSNL-1 fragment are shown. (B) Purified recombinant GSNL-1 variants (0.5 μg each) were subjected to SDS−PAGE and stained with Coomassie Brilliant Blue. Molecular mass markers (M) in kilodaltons are shown at the left of the gel.

have distinct roles in actin regulatory activities with similarities and differences from those of gelsolin. These results provide interesting information about the conservation and diversity of utilization of G domains in gelsolin-related proteins.

EXPERIMENTAL PROCEDURES

Proteins and Materials. Actin was purified from rabbit skeletal muscle acetone powder (Pel-Freeze Biologicals) as described previously (*19*). Pyrene-labeled actin was prepared as described previously (*20*). Bacterially expressed full-length GSNL-1 was purified as described previously (*18*). Phosphatidylinositol 4,5-bisphosphate (PIP2) (P-4516, Echelon Biosciences) was suspended in water at 1 mg/mL with brief sonication and stored at −20 °C.

Production of Truncation Mutants of GSNL-1. Fragments of GSNL-1 cDNA encoding truncated GSNL-1 sequences as shown in Figure 1 were amplified by polymerase chain reaction from pGEX-GSNL-1 (*18*) as a template and cloned into pGEX-2T between the BamHI and SmaI sites using an Infusion PCR Cloning Kit (Clontech). The sequences of the inserts were verified by DNA sequencing. *Escherichia coli* strain BL21(DE3) was transformed with the expression vectors and cultured in M9ZB (18.7 mM NaH_4Cl, 22 mM KH_2PO_4, 42.3 mM Na_2HPO_4, 1% tryptone, 85.6 mM NaCl, 1 mM $MgSO_4$, and 0.4% glucose) containing 50 μg/mL ampicillin at 37 °C until the A_{600} reached 0.6 cm^{-1}. Then, the cultures were cooled to room temperature, and expression was induced via addition of 0.1 mM isopropyl 1-thio-β-D-galactopyranoside for 2 h at room temperature. The cells were harvested by centrifugation at 5000*g* for 10 min and homogenized with a French pressure cell at 360−580 kg/cm^2 in phosphate-buffered saline (137 mM NaCl, 2.7 mM KCl, 1.4 mM KH_2PO_4, and 8 mM Na_2HPO_4). The homogenates were centrifuged at 20000*g* for 15 min, and the supernatants were applied to a glutathione Uniflow (Clontech) column (1.5 mL bed volume). After the samples had been washed with phosphate-buffered saline, 15 units of thrombin (Roche Applied Science) was added to cleave the N-terminal glutathione *S*-transferase (GST) tag, and GSNL-1 truncation mutants were eluted from the column. They were dialyzed against F buffer [0.1 M KCl, 2 mM $MgCl_2$, and 20 mM HEPES-NaOH (pH 7.5)] containing 50% glycerol and stored at −20 °C. Protein concentrations were determined by densitometry of Coomassie blue-stained gels after SDS−PAGE using actin as a standard.

Labeling of Actin by DyLight549. Four milliliters of polymerized actin at 4 mg/mL in a buffer containing 0.1 M KCl, 20 mM $NaHCO_3$, 2 mM $MgCl_2$, 0.2 mM ATP, and 0.2 mM dithiothreitol was mixed with 100 μL of 10 mg/mL DyLight 549 NHS ester (Pierce/Thermo Scientific) in dimethylformamide and incubated overnight on ice. F-Actin was sedimented by ultracentrifugation at 100000 rpm for 1 h with a Beckman TLA100.3 rotor, and suspended in 2 mL of G buffer containing 0.2 mM $CaCl_2$, 0.2 mM ATP, 0.2 mM dithiothreitol, and 2 mM Tris-HCl (pH 8.0). After brief sonication, it was dialyzed against G buffer overnight to depolymerize actin and to remove unincorporated DyLight 549. Then, the remaining F-actin was removed by ultracentrifugation at 100000 rpm for 1 h by a Beckman TLA100.3 rotor, and the supernatant was applied to gel filtration using Sephacryl S-300 (HiPrep 26/60, GE Healthcare) equilibrated with G buffer. Fractions containing G-actin were pooled and concentrated by a Vivaspin 15R centrifugal concentrator (MWCO of 10000) to ~40 μM actin. The concentration of actin was determined spectrophotometrically using an extinction coefficient of 0.63 mg^{-1} mL cm^{-1} at 290 nm. The molar ratio of bound DyLight 549 to actin was 0.65, which was determined using the manufacturer's instructions. DyLight 549-labeled G-actin was snap-frozen in small aliquots and stored at −80 °C.

Direct Observation of Actin Filaments by Fluorescence Microscopy. Unlabeled G-actin was copolymerized with DyLight 549-labeled G-actin at 2 μM total actin (20% labeled) for 2 h in F buffer. Labeled actin was diluted to 0.4 μM in F buffer with or without GSNL-1 variants in the presence of 0.1 mM $CaCl_2$ or 5 mM EGTA and incubated for 5 min at room temperature. Then, the reaction mixtures were put on a nitrocellulose-coated coverslip, and immobilized actin filaments on the coverslip were observed by epifluorescence using a Nikon TE2000 microscope with a 60× Plan Apo objective (oil, numerical aperture of 1.4). Micrographs were captured with a SPOT RT Monochrome CCD camera (Diagnostic Instruments) and processed with IPLab (BD Biosciences) and Adobe Photoshop CS2.

Determination of the Critical Concentration of Actin. Varying concentrations of pyrene-labeled G-actin (20% labeled) were polymerized overnight at room temperature in the presence of constant concentrations of GSNL-1 fragments in F buffer containing 0.1 mM $CaCl_2$ or 5 mM EGTA. The fluorescence intensity of pyrene (excitation at 366 nm and emission at 384 nm) at the steady state was measured with a Perkin-Elmer LS50B fluorescence spectrophotometer.

F-Actin Cosedimentation Assays. F-Actin cosedimentation assays were performed as described previously (*21*) with some modifications. Varying concentrations of GSNL-1 variants were added to 5 μM F-actin in F buffer with 0.2 mM dithiothreitol and 0.1 mM $CaCl_2$ or 0.1 mM EGTA. After incubation for 1 h at room temperature, the mixtures were ultracentrifuged with a Beckman TLA100 rotor at 436000*g* for 15 min at 20 °C. Supernatant and pellet fractions were adjusted to the same volumes and subjected to SDS−PAGE and staining with Coomassie Brilliant Blue R-250 (National Diagnostics). Gels were scanned with an Epson Perfection V700 Photo Scanner at 300 dots per inch, and band intensity was quantified using Image J. To assess the cosedimentation of GSNL-1 variants with F-actin, experiments were performed in the absence of actin, and actin-independent sedimentations of GSNL-1 variants were quantified and subtracted from the experimental data in the presence of actin.

Nondenaturing Polyacrylamide Gel Electrophoresis. Nondenaturing polyacrylamide gel electrophoresis for examining G-actin binding and PIP2 binding was performed as described previously (*22*, *23*). GSNL-1 variants were incubated with G-actin or PIP2 in G buffer for 30 min at room temperature. The samples were supplemented with 0.25 volume of a loading buffer (50% glycerol and 0.05% bromophenol blue) and electrophoresed using a Bicine/triethanolamine buffer system at 4 °C. The proteins were visualized after being stained with Coomassie Brilliant Blue R-250 (National Diagnostics).

Analytical Gel Filtration Chromatography. A Superdex 75 10/300 GL gel filtration column (24 mL bed volume, GE Healthcare) was equilibrated with F buffer containing 0.2 mM dithiothreitol and 0.1 mM $CaCl_2$, and proteins at 1 mg/mL (500 μL) were applied and eluted with the same buffer. The eluates were collected in fractions of 0.5 mL each and analyzed by SDS−PAGE and staining with Coomassie Brilliant Blue R-250. Gels were scanned with an Epson Perfection V700 Photo Scanner at 300 dots per inch, and band intensity was quantified using Image J. Bovine serum albumin (66 kDa) (A8531, Sigma-Aldrich) and bovine carbonic anhydrase (29 kDa) (C7025, Sigma-Aldrich) were used as molecular mass standards.

RESULTS

Construction of Truncation Mutants of GSNL-1 for Domain Mapping. To dissect functional domains of GSNL-1, we produced five truncation mutants containing different G domains as shown in Figure 1. Each G domain was truncated from the C-terminus to generate G1G2G3, G1G2, and G1. We made two G1 variants with (G1b) or without (G1a) a linker between G1 and G2 (Figure 1A) because a homologous region of gelsolin is implicated in actin filament severing activity (*8*, *24*, *25*). We also made G3G4, which lacks two N-terminal G domains. These GSNL-1 fragments were expressed in *E. coli* as fusion proteins with GST and purified after the GST tag had been removed (Figure 1B). We also tested bacterial expression of a mutant lacking only the C-terminal tail of 16 amino acids and a fragment containing G2G3G4, but these recombinant proteins were insoluble and not functionally tested in this study (our unpublished data).

Actin Filament Severing. GSNL-1 severs actin filaments in a Ca^{2+}-dependent manner (*18*). The F-actin severing activity of GSNL-1 truncation mutants was examined by direct microscopic observation of fluorescently labeled actin filaments. DyLight 549-labeled actin filaments were incubated with GSNL-1 variants in the presence or absence of calcium, immobilized on a nitrocellulose-coated coverslip, and observed by fluorescence microscopy. Control experiments with actin filaments with buffer only showed long filaments (Figure 2A,B). At 20 nM GSNL-1 mutants, G1G2G3 (Figure 2E), G1G2 (Figure 2G), and G1b (Figure 2I) fragmented actin filaments in the presence of Ca^{2+} as well as full-length GSNL-1 (Figure 2C) but not in the presence of EGTA (Figure 2F,H,J). Although G1a did not sever actin filaments at 20 nM (Figure 2K,L), it exhibited severing activity at higher concentrations. The concentration of G1a needed to be increased to 2−5 μM to achieve filament severing to an extent similar to that of 20 nM full-length GSNL-1 (data not shown), indicating that G1a was > 100-fold weaker in actin severing than full-length GSNL-1, G1G2G3, G1G2, and G1b. It should be noted that the difference between G1a and G1b is the absence or presence of the G1−G2 linker sequence (16 amino acids) (Figure 1A), indicating that this region is critical for actin filament severing. G3G4 did not sever actin filaments (Figure 2M,N). These results indicate that G1 and the linker between G1 and G2 play critical roles in actin filament severing.

Barbed End Capping. GSNL-1 caps the barbed end of the actin filament in a Ca^{2+}-dependent manner (*18*). Barbed end capping activity was tested by effects of GSNL-1 truncation mutants on the critical concentration (C_c) of actin. The C_c of actin with free ends is generally 0.1−0.2 μM. Since the C_c at the barbed end (0.1 μM) is much lower than that at the pointed end (0.5 μM), the C_c of barbed-end-capped actin will be near the C_c value at the pointed end (0.5 μM). In the presence of Ca^{2+}, full-length GSNL-1 shifted the C_c to ∼0.4 μM [Figure 3A (○)], indicating that it capped the barbed end. G1G2G3 [Figure 3A (▼)] and G1G2 [Figure 3A (△)] similarly shifted the C_c to ∼0.4 μM in the presence of Ca^{2+}. However, G1a [Figure 3A (□)], G1b [Figure 3A (■)], and G3G4 [Figure 3A (◆)] did not alter the C_c. All tested GSNL-1 fragments did not alter C_c in the absence of Ca^{2+} (Figure 3B). Thus, G1G2 is sufficient for Ca^{2+}-dependent barbed end capping. The lack of capping activity of G1a and G1b suggests that G2 is important for barbed end capping.

G-Actin Binding. G-Actin binding activity was examined by nondenaturing polyacrylamide gel electrophoresis. Full-length GSNL-1 binds to G-actin in the presence of calcium (*18*), and the complex of GSNL-1 and G-actin appeared as bands with a mobility slower than those of GSNL-1 and actin (Figure 4A). In the absence of calcium, no extra bands were detected in the mixtures of GSNL-1 and G-actin (Figure 4B), indicating that this interaction is calcium-dependent. In the presence of calcium, all the tested GSNL-1 fragments bound to G-actin (Figure 4C,E,G, I,K). For G1G2G3 (Figure 4C) and G3G4 (Figure 4K), although bands of the complexes were not clearly detected, the magnitude of the band of actin was diminished when the concentrations of G1G2G3 or G3G4 were increased, suggesting that the complexes of G-actin and G1G2G3 or G3G4 migrated differently than G-actin alone but did not focus in distinct bands. For G1G2 (Figure 4E) and G1b (Figure 4G), bands of the complex appeared above the band of G1G2 or G1b with increasing concentrations of the fragments. G1a did not apparently alter the mobility of the actin band (Figure 4I). However, the band of G1a, which was resolved in two bands, disappeared in the presence of G-actin, suggesting that the G1a−G-actin complex migrated at the same location as G-actin alone.

In the absence of calcium, G1G2G3 (Figure 4D) and G3G4 (Figure 4L) bound to G-actin, while G1G2 (Figure 4F), G1b

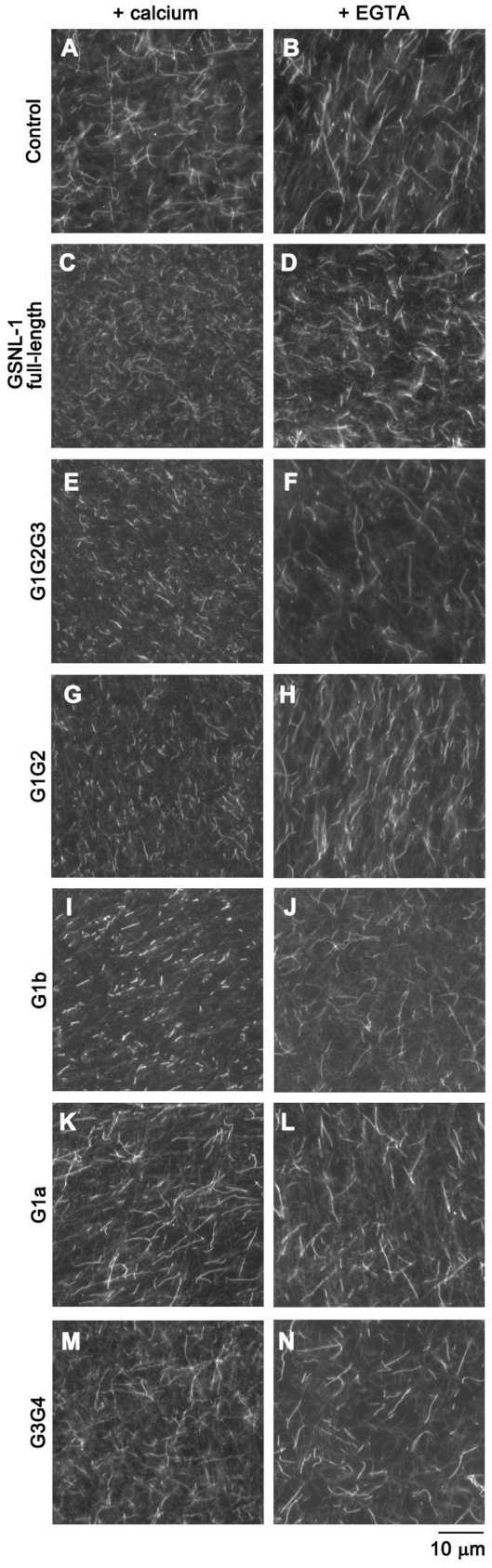

FIGURE 2: Direct observation of actin filament severing by fluorescence microscopy. DyLight 549-labeled actin filaments were incubated with buffer only (control) (A and B), 20 nM full-length GSNL-1 (C and D), 20 nM G1G2G3 (E and F), 20 nM G1G2 (G and H), 20 nM G1b (I and J), 20 nM G1a (K and L), or 20 nM G3G4 (M and N) in the presence of 0.1 mM $CaCl_2$ (left column) or 5 mM EGTA (right column) for 5 min, and the filaments were observed by fluorescence microscopy. The bar is 10 μm.

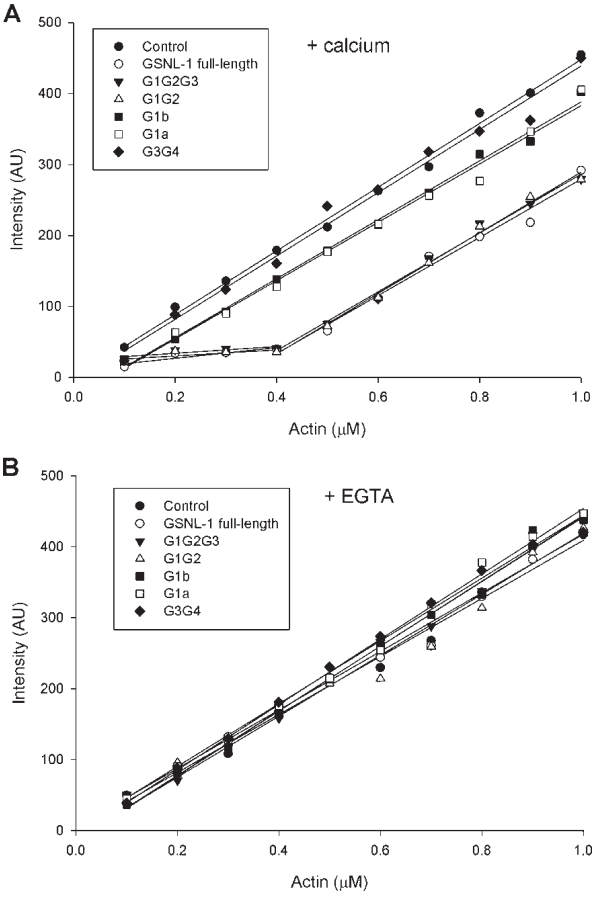

FIGURE 3: Effects of GSNL-1 variants on the critical concentration of actin. Varying concentrations (0.1−1.0 μM) of 20% pyrene-labeled actin were polymerized with or without 50 nM GSNL-1 variants in the presence of 0.1 mM $CaCl_2$ (A) or 5 mM EGTA (B). After overnight incubation, the pyrene fluorescence (arbitrary units) was measured and plotted as a function of the total actin concentration.

(Figure 4H), and G1a (Figure 4I) did not. G1G2G3 (Figure 4D) and G3G4 (Figure 4L) caused shifts in the band of actin in the presence of EGTA as well as in the presence of calcium (Figure 4C,K). Therefore, G1G2G3 and G3G4 bound to G-actin in a calcium-independent manner. In contrast, no alterations were detected in the band patterns of G-actin and GSNL-1 fragments for mixtures of G-actin with G1G2 (Figure 4F), G1b (Figure 4H), or G1a (Figure 4J) in the presence of EGTA. Thus, these GSNL-1 fragments bound to G-actin in a calcium-dependent manner. Overall, these results suggest that GSNL-1 has at least two G-actin-binding sites, a calcium-dependent site in G1 and a calcium-independent site in G3G4.

Native Molecular Mass. Our nondenaturing electrophoresis analysis of GSNL-1 variants and actin demonstrated that several variants were resolved in multiple bands as GSNL-1 variants themselves or in complex with actin (Figure 4). We previously showed that multiple bands of the full-length GSNL-1−actin complex contain a 1:1 molar ratio of GSNL-1 to actin (*18*), but our analysis did not preclude the possibility that GSNL-1 and actin formed oligomers containing the same numbers of each molecule. We attempted to determine the native molecular mass of the full-length GSNL-1−actin complex in G buffer by gel filtration chromatography. However, our attempts failed due to nonspecific interactions between the protein and the gel matrices under low-ionic strength conditions in G buffer (our unpublished data). Therefore, we estimated the native molecular mass

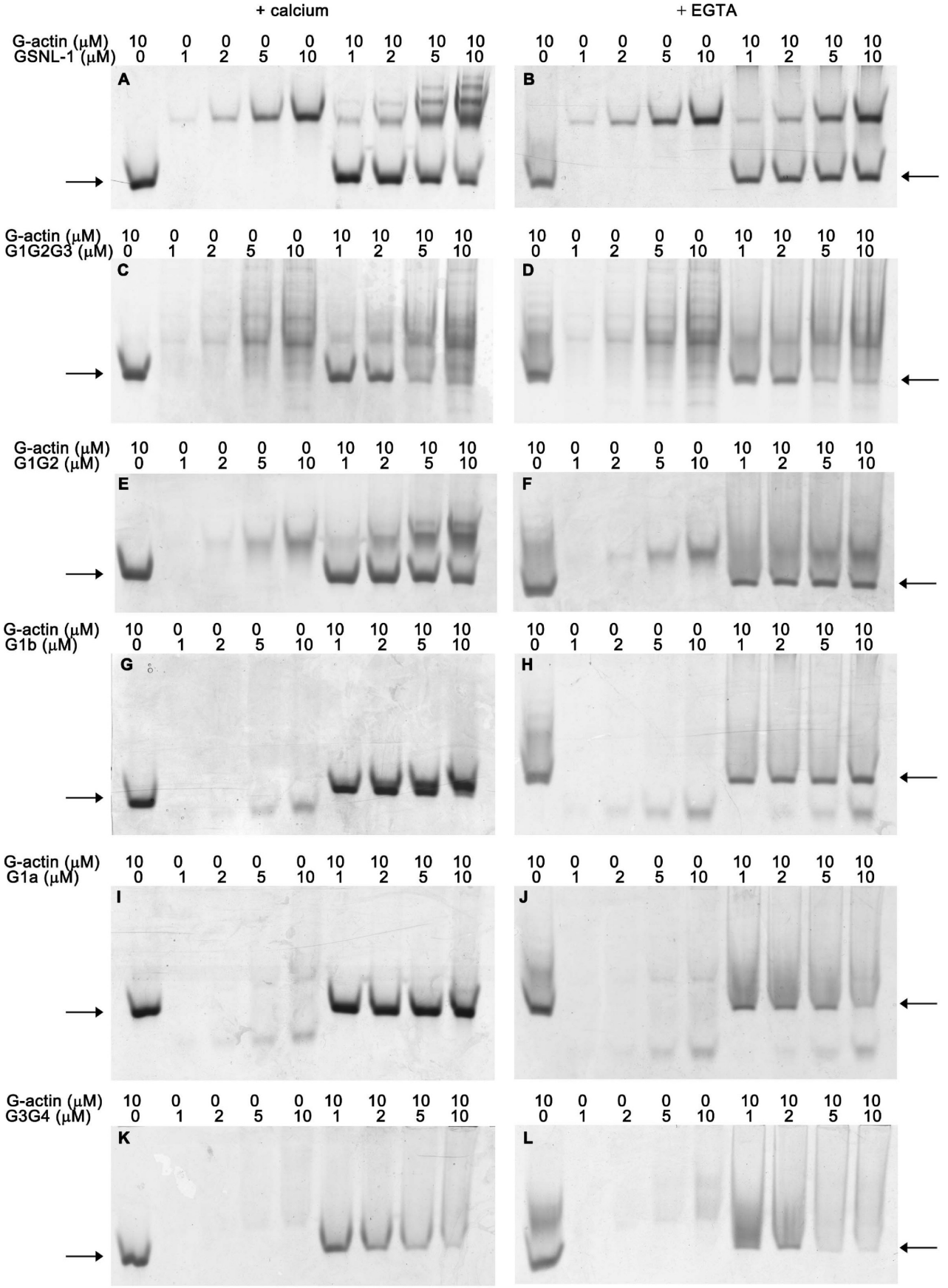

FIGURE 4: Examination of G-actin binding by GSNL-1 variants by nondenaturing polyacrylamide gel electrophoresis. G-Actin (10 μM) and varying concentrations (0−10 μM) of full-length GSNL-1 (A and B), G1G2G3 (C and D), G1G2 (E and F), G1b (G and H), G1a (I and J), or G3G4 (K and L) were incubated alone or in mixtures in the presence of 0.1 mM $CaCl_2$ (left column) or 0.5 mM EGTA (right column) for 30 min, and the samples were analyzed by nondenaturing polyacrylamide gel electrophoresis. Positions of free G-actin are indicated by arrows.

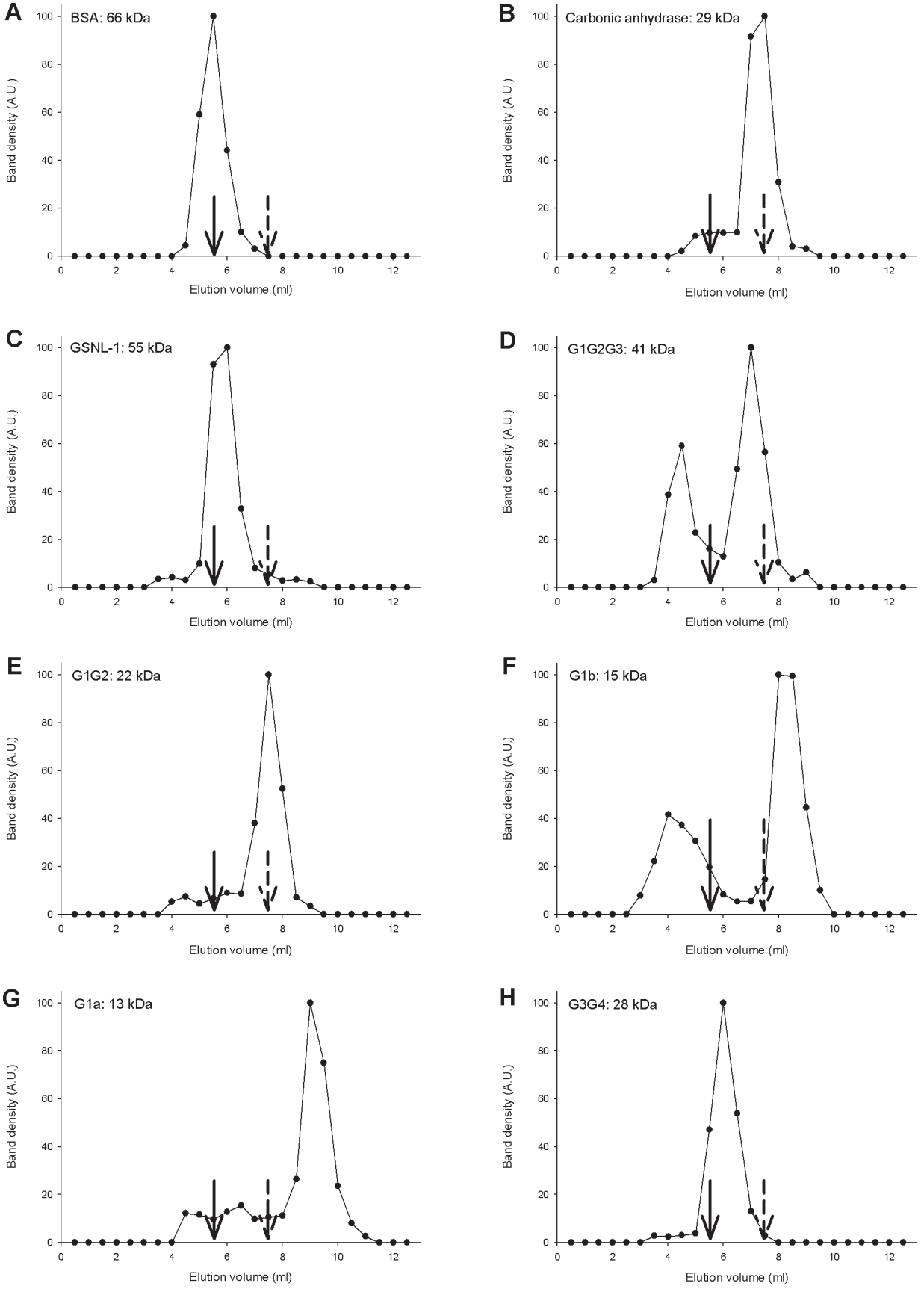

FIGURE 5: Estimation of the native molecular mass of GSNL-1 variants by gel filtration chromatography. Bovine serum albumin (BSA) (A), carbonic anhydrase (CA) (B), GSNL-1 (C), G1G2G3 (D), G1G2 (E), G1b (F), G1a (G), or G3G4 (H) was applied to a Superdex 75 gel filtration column (24 mL bed) and eluted with F buffer containing 0.1 mM $CaCl_2$. The eluates were fractionated every 0.5 mL, and eluted proteins were analyzed by SDS−PAGE and Coomassie blue staining. The density of the protein bands (arbitrary units) was plotted as a function of elution volume (milliliter). Arrows with solid lines and broken lines indicate peak positions of BSA (66 kDa) and CA (29 kDa), respectively. Molecular masses shown in the figure are calculated values for monomers.

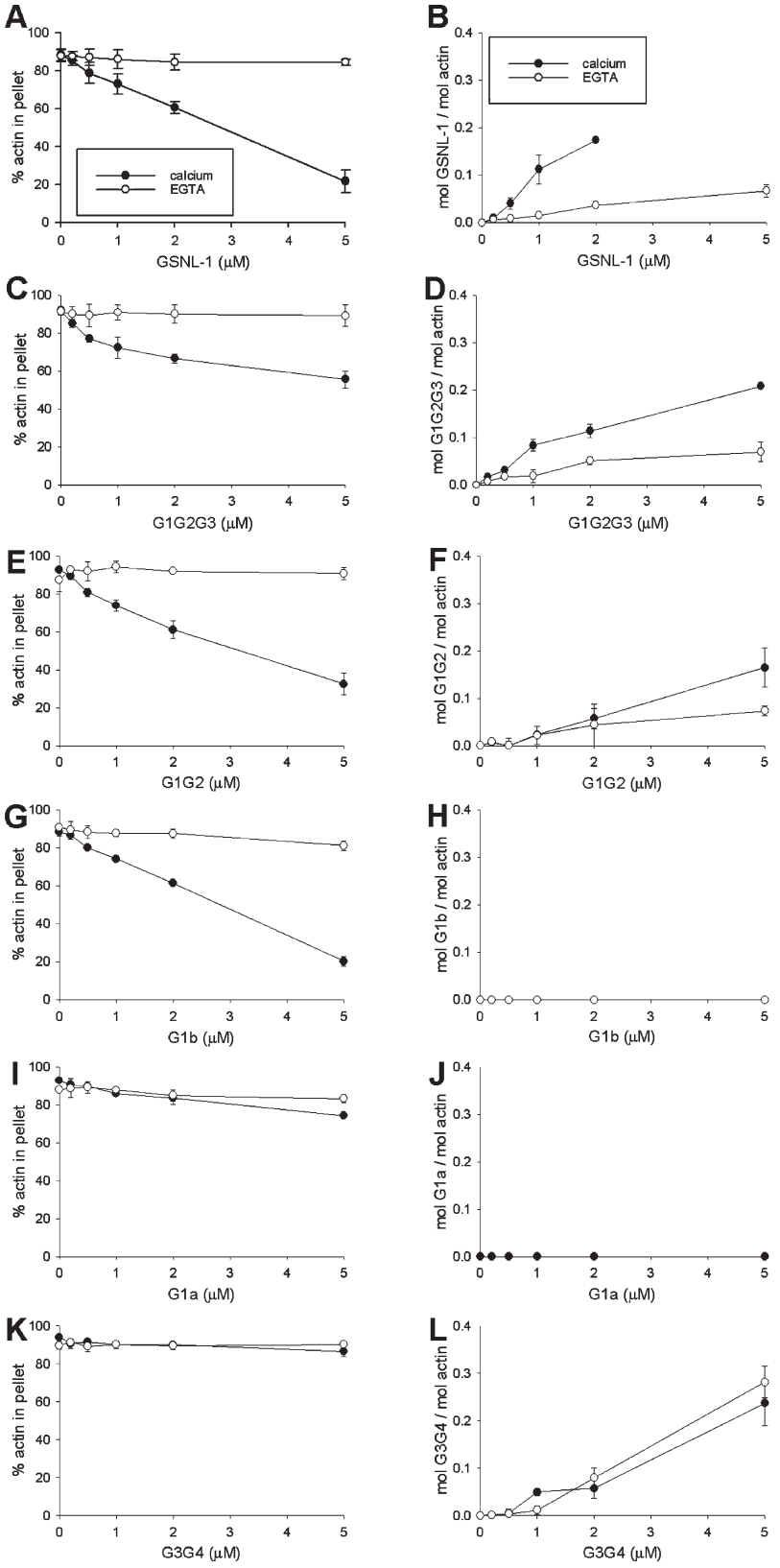

FIGURE 6: Cosedimentation assays of GSNL-1 variants with F-actin. F-Actin (5 μM) was incubated with varying concentrations (0−5 μM) of full-length GSNL-1 (A and B), G1G2G3 (C and D), G1G2 (E and F), G1b (G and H), G1a (I and J), or G3G4 (K and L) in the presence of 0.1 mM $CaCl_2$ (●) or 0.1 mM EGTA (○) for 1 h and ultracentrifuged at 436000*g* for 15 min. The supernatants and pellets were separated and analyzed by SDS−PAGE. Band intensities were quantified by densitometry, and actin-independent sedimentations of GSNL-1 variants were subtracted from the experimental data in the presence of actin. In the left column (A, C, E, G, I, and K), the percentages of actin in the pellet fractions are plotted as a function of the total concentrations of GSNL-1 variants. In the right column (B, D, F, H, J, and L), molar ratios of GSNL-1 variants to actin in the pellets are plotted as a function of the total concentrations of GSNL-1 variants. Data are averages ± standard deviations of three experiments.

of GSNL-1 fragments alone in F buffer in the presence of calcium by gel filtration chromatography using Superdex 75 (Figure 5). As molecular mass standards, bovine serum albumin (BSA) (66 kDa) and carbonic anhydrase (CA) (29 kDa) were eluted

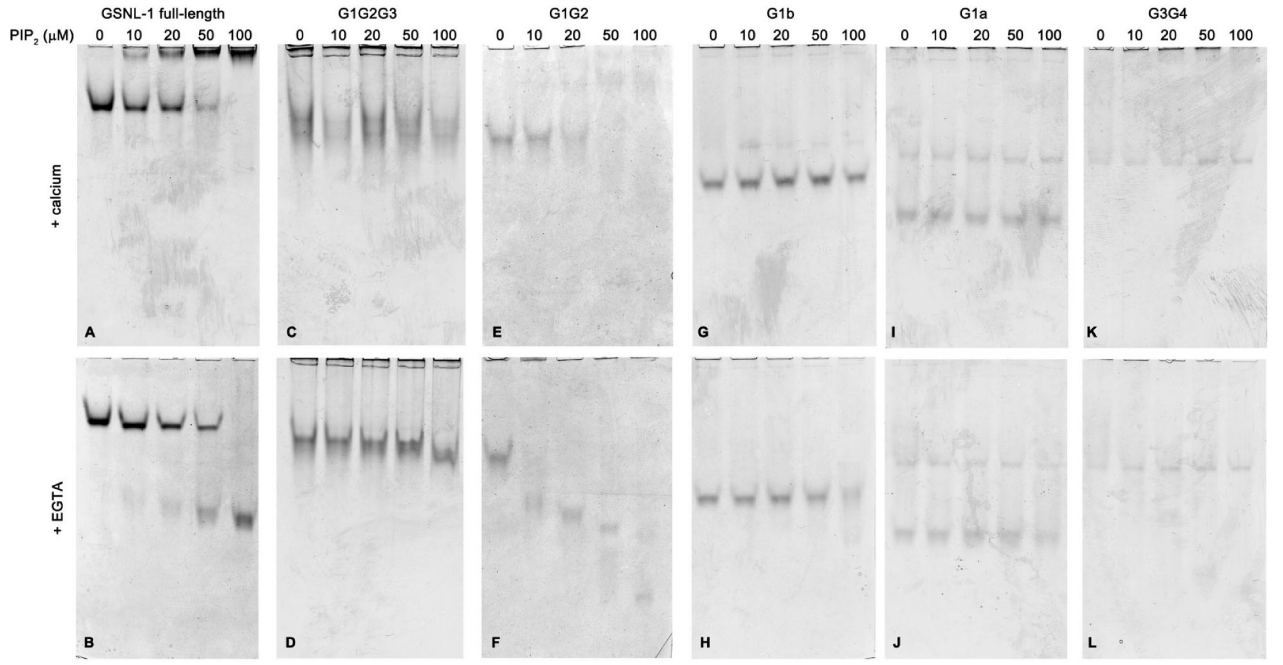

FIGURE 7: Examination of PIP2 binding by GSNL-1 variants by nondenaturing polyacrylamide gel electrophoresis. Full-length GSNL-1 (A and B), G1G2G3 (C and D), G1G2 (E and F), G1b (G and H), G1a (I and J), or G3G4 (K and L) at 5 μM was incubated with varying concentrations (0−100 μM) of PIP2 in G buffer in the presence of 0.1 mM $CaCl_2$ (A, C, E, G, I, and K) or 0.5 mM EGTA (B, D, F, H, J, and L) for 30 min, and the samples were analyzed by nondenaturing polyacrylamide gel electrophoresis.

at 5.5 and 7.5 mL, respectively (Figure 5A,B). Full-length GSNL-1 (55 kDa) was eluted as a single peak at ~6.0 mL that is near but slightly slower than the peak of BSA (66 kDa) (Figure 5C), indicating that GSNL-1 is a monomer. Similarly, G1G2 (Figure 5E) and G1a (Figure 5G) were eluted as single peaks that corresponded to elution volumes of monomers. G1G2G3 was eluted as two major peaks of estimated dimer (82 kDa) and monomer (41 kDa) (Figure 5D), suggesting that multiple bands of G1G2G3 in nondenaturing electrophoresis (Figure 4C, D) are partly due to mixed dimeric and monomeric states. G1b was also eluted as two peaks, with one peak with a large molecular mass and another peak that corresponded to the monomer (15 kDa) (Figure 5F). Since the peak of large molecular mass is broad and estimated to be much larger than the calculated mass of the G1b tetramer (60 kDa), this peak likely represents oligomers or aggregates of G1b. Interestingly, G3G4 was eluted as a single peak at 6.0 mL that is closer to BSA (66 kDa) than CA (29 kDa) (Figure 5H), suggesting that G3G4 is a constitutive dimer (56 kDa). However, a smear appearance of G3G4 in nondenaturing electrophoresis (Figure 4K,L) suggests that G3G4 is present as either a monomer or a dimer with variable conformational states under low-ionic strength conditions in G buffer.

F-Actin Binding. GSNL-1 binds to actin filaments in a calcium-dependent manner (*18*). F-Actin binding of full-length GSNL-1 and GSNL-1 fragments was examined by cosedimentation assays (Figure 6). Full-length GSNL-1 cosedimented with F-actin in a calcium-dependent manner as previously shown (Figure 6B). We were not able to quantify cosedimentation of GSNL-1 with actin at a high GSNL-1 concentration (5 μM) because of large deviations in the data. It also decreased the level of pelletable actin in a calcium-dependent manner (Figure 6A), which indicates an increase in the level of fragmented short filaments. G1G2G3 had slightly weaker calcium-dependent actin fragmentation (Figure 6C) and F-actin binding activities (Figure 6D) than full-length GSNL-1 (Figure 6A,B). G1G2 induced calcium-dependent actin fragmentation nearly as strongly as full-length GSNL-1 (Figure 6E) and very weak cosedimentation with F-actin (Figure 6F). Since there was little cosedimentation of G1G2 with F-actin, it may simply represent its association with actin-barbed ends but not with the side of filaments. Either G1b (Figure 6H) or G1a (Figure 6J) did not bind to F-actin. However, G1b (Figure 6G), but not G1a (Figure 6I), fragmented actin filaments as strongly as full-length GSNL-1 (Figure 6A), which is consistent with the microscopic observations (Figure 2). On the other hand, G3G4 cosedimented with F-actin in the presence or absence of calcium (Figure 6L) and showed no actin fragmentation activity (Figure 6K). These results suggest that GSNL-1 has a calcium-independent F-actin binding site in G3G4. However, a regulatory site for calcium-sensitive F-actin binding activity still needs to be determined.

Phosphoinositide Binding. Gelsolin and gelsolin-related proteins directly bind to phospholipids, including phosphatidylinositol 4,5-bisphosphate (PIP2) (*26*−*28*). By nondenaturing gel electrophoresis, we found that full-length GSNL-1 directly binds to PIP2 (Figure 7A,B). With an increase in the concentrations of PIP2, the band of GSNL-1 was shifted to an upper band in the presence of calcium (Figure 7A) or a lower band in the presence of EGTA (Figure 7B). Bands of G1G2G3 were not modified by PIP2 in the presence or absence of calcium (Figure 7C,D), suggesting that it did not bind to PIP2 or that the interaction was too weak to be detected by electrophoresis. In contrast, the band shift of G1G2 occurred at much lower PIP2 concentrations than that of full-length GSNL-1 (compare panels A and E of Figure 7), suggesting that G1G2 binds to PIP2 with a higher affinity than full-length GSNL-1. G1G2 bound to PIP2 with an even higher affinity in the presence of EGTA (Figure 7F) than in the presence of calcium (Figure 7E). Thus, removal of G3 from G1G2G3 greatly augmented PIP2 binding, suggesting that G3 has an inhibitory role in PIP2 binding. G1b did not interact with

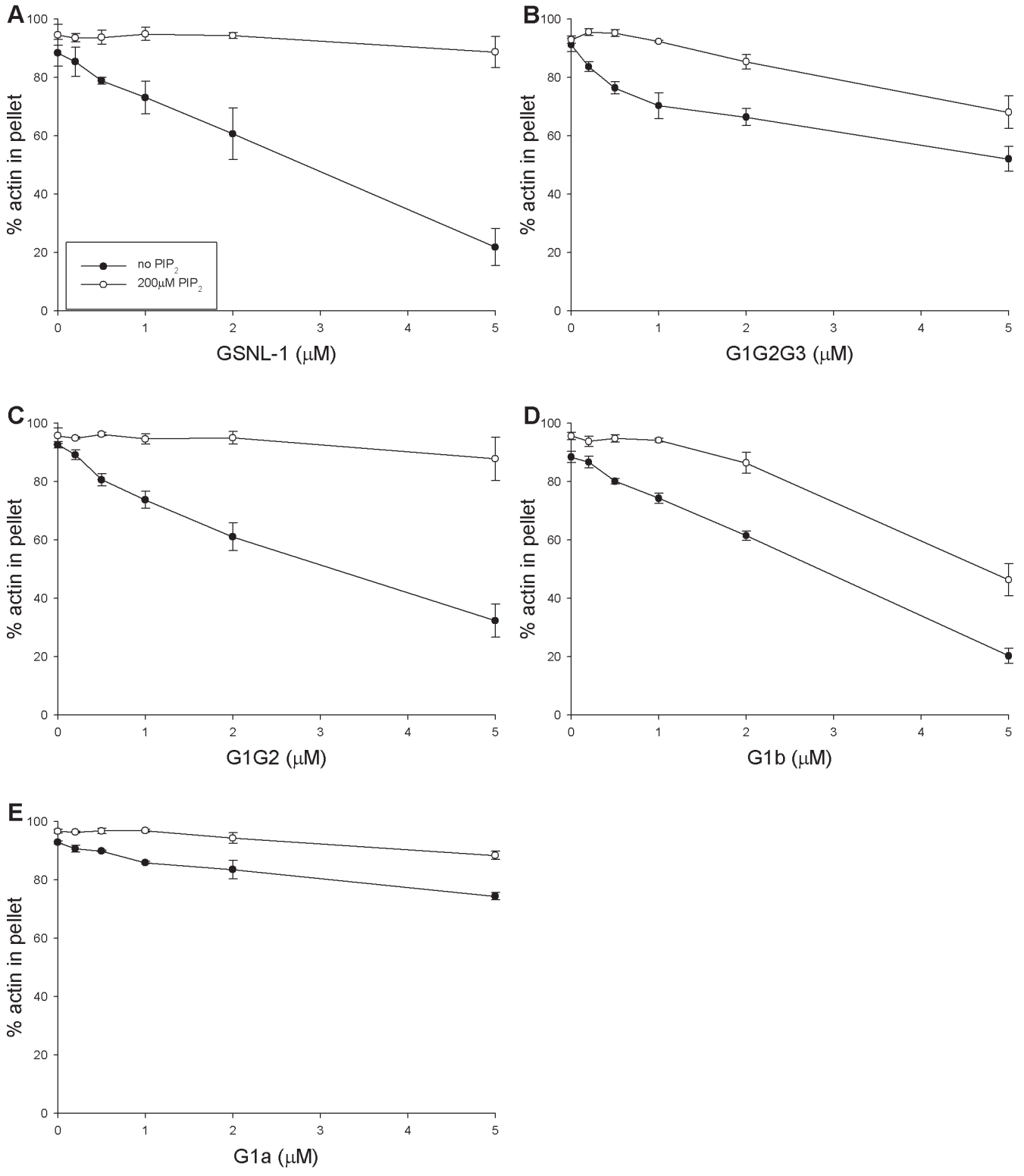

FIGURE 8: Effects of PIP2 on actin fragmentation by GSNL-1 variants. F-Actin (5 μM) was incubated with varying concentrations (0−5 μM) of full-length GSNL-1 (A), G1G2G3 (B), G1G2 (C), G1b (D), or G1a (E) in the presence of 0.1 mM $CaCl_2$ with (○) or without (●) 200 μM PIP2 for 30 min and ultracentrifuged at 436000*g* for 15 min. The supernatants and pellets were separated and analyzed by SDS−-PAGE. Band intensities were quantified by densitometry, and percentages of actin in the pellet fractions were plotted as a function of the total concentrations of GSNL-1 variants. Data are averages ± standard deviations of three experiments.

PIP2 in the presence of calcium (Figure 7G), while a weak band shift was detected for G1b in the presence of EGTA at 100 μM PIP2 (Figure 7H). No PIP2-induced band shift was observed for G1a (Figure 7I,J) or G3G4 (Figure 7K,L), suggesting that these fragments did not bind to PIP2 or that the interactions were too weak to be detected by electrophoresis. These results indicate that G2 is necessary for PIP2 binding and that PIP2 binding is attenuated in G1G2G3.

Binding of PIP2 to GSNL-1 inhibited its F-actin fragmentation activity as demonstrated by actin sedimentation assays (Figure 8). GSNL-1 fragmented actin filaments in the absence of PIP2 and decreased the level of pelletable actin [Figure 8A (●)].

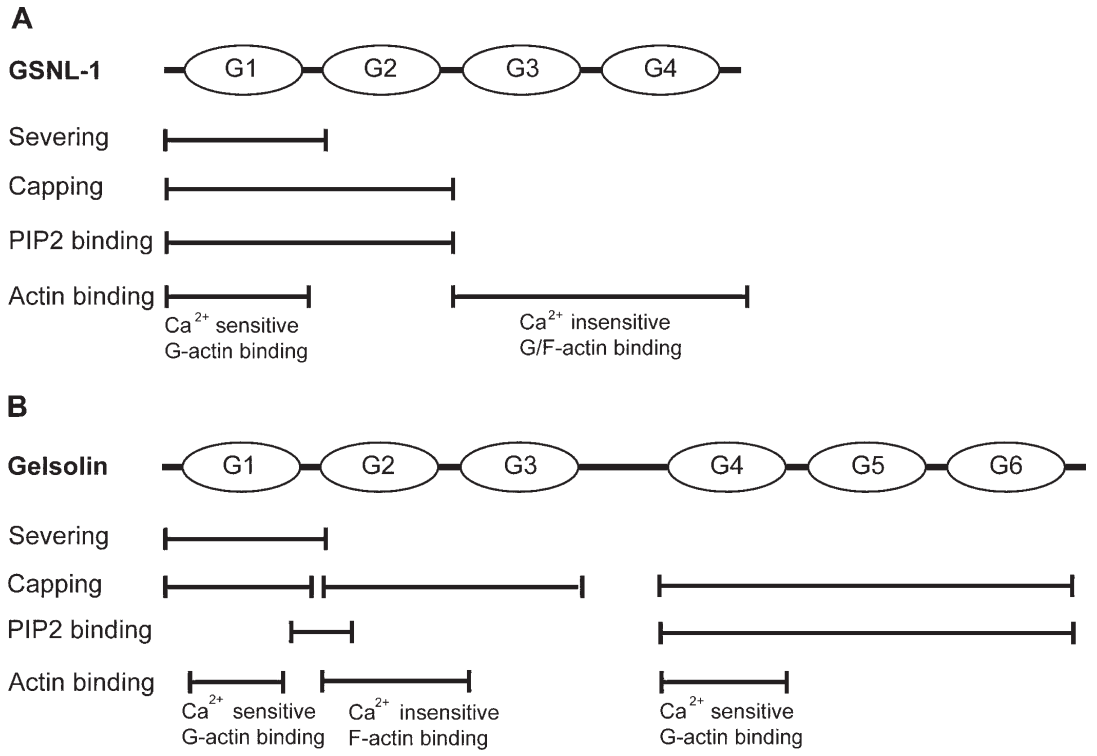

FIGURE 9: Comparison of functional domains between *C. elegans* GSNL-1 and mammalian gelsolin. (A) Functional domains of *C. elegans* GSNL-1 identified in this study. (B) Functional domains of mammalian gelsolin were adapted from Sun et al. (*2*), with modifications based on the following references: severing (*8*), capping (*9*, *31*), PIP2 binding (*32*, *33*, *36*), calcium-sensitive G-actin binding in G1 (*37*), calcium-insensitive F-actin binding in G2 (*31*), and calcium-sensitive G-actin binding in G4 (*38*).

Table 1: Summary of Properties of GSNL-1 Variants

	GSNL-1	G1G2G3	G1G2	G1b	G1a	G3G4
amino acid residues	1−475	1−353	1−239	1−131	1−115	240−475
filament severing						
with Ca^{2+}	++	++	++	++	+	−
without Ca^{2+}	−	−	−	−	−	−
capping						
with Ca^{2+}	+	+	+	−	−	−
without Ca^{2+}	−	−	−	−	−	−
G-actin binding						
with Ca^{2+}	+	+	+	+	+	+
without Ca^{2+}	−	+	−	−	−	+
F-actin binding						
with Ca^{2+}	+	+	±	−	−	+
without Ca^{2+}	−	−	−	−	−	+
PIP2 binding						
with Ca^{2+}	+	−	+	−	−	−
without Ca^{2+}	+	−	+	±	−	−
PIP2 regulation						
with Ca^{2+}	++	+	++	+	+	not determined

However, in the presence of 200 μM PIP2, full-length GSNL-1 did not show F-actin fragmentation [Figure 8A (○)]. Similarly, activity of G1G2 was fully inhibited by PIP2 (Figure 8C) as well as full-length GSNL-1. In contrast, activity of G1G2G3 (Figure 8B), G1b (Figure 8D), or G1a (Figure 8E) was only weakly inhibited by PIP2 (Figure 8B). These results are consistent with the PIP2 binding properties of GSNL-1 variants (Figure 7). Full-length GSNL-1 and G1G2 bound to PIP2 strongly and were effectively inhibited by PIP2, whereas G1b only weakly bound to PIP2 and was not strongly inhibited by PIP2. Activities of G1G2G3 and G1b were weakly inhibited by PIP2, whereas they did not show binding with PIP2 in nondenaturing electrophoresis, suggesting that binding of G1G2G3 or G1b to PIP2 was too unstable to be detected by electrophoresis. These results suggest that G2 is required for both PIP2 binding and PIP2 sensitivity.

DISCUSSION

In this study, dissection of functional domains of GSNL-1 identified distinct functions of the four gelsolin-like repeats and revealed similarities and differences between GSNL-1 and gelsolin in utilizing these domains to regulate actin dynamics (Figure 9 and Table 1). Remarkably, only G1, the N-terminal G domain, with a linker between G1 and G2 was sufficient for nearly full actin filament severing activity, whereas G2 was required for barbed end capping and PIP2 binding (Figure 9A). At least two actin-binding sites were identified: one in G1 that binds to G-actin in the presence of calcium and the other in G3G4 that binds to both G- and F-actin in a manner independent of calcium (Figure 9A). These results show that the essential function of the N-terminal G domain (G1) in actin filament severing is conserved between GSNL-1 and gelsolin, but roles of other G domains in barbed end capping and PIP2 binding are diverged. Thus, GSNL-1 and gelsolin are conserved in the actin filament severing and capping activities but with differential utilization of G domains.

G1 with a linker between G1 and G2 (G1b) is the smallest GSNL-1 fragment that exhibits strong calcium-dependent actin filament severing activity (Figure 9A and Table 1). G1 without the G1−G2 linker (G1a) had only weak severing activity. Similar observations have been reported for gelsolin (Figure 9B) (*8*). Kwiatkowski et al. demonstrated that a gelsolin fragment (PG160) containing G1 and a short G1−G2 linker sequence had nearly full severing activity while a shorter fragment (PG149) lacking the linker sequence had very weak severing activity (*8*). G1 of gelsolin binds to actin at a cleft between subdomains

1 and 3 (*11*). The amino acid sequence of the G1−G2 linker of gelsolin contains a similarity with that of WASP homology 2 (*29*) and plays an important role in actin filament severing (*8*, *24*, *25*). The crystal structure of gelsolin fragment PG160 in complex with G-actin shows that the G1−G2 linker makes a close contact with the surface of actin at residues 24−30 (*29*). Thus, the interaction between the G1−G2 linker and actin may promote or stabilize binding of G1 to actin and enhance its severing activity. On the basis of the sequence similarity, G1 and the G1−G2 linker of GSNL-1 most likely bind to the actin monomer in a manner similar to that of the equivalent region of gelsolin. The G1−G2 linker of G1b perhaps enhances binding to F-actin, but G1b did not cosediment with F-actin (Figure 6H). This might be due to instantaneous severing and disassembly of F-actin after association of G1b with F-actin. Therefore, the role of the G1−G2 linker of GSNL-1 needs to be investigated with other techniques with higher temporal resolution. Functions of other G domains are different between GSNL-1 and gelsolin. G1b, G1G2, and G1G2-G3 of GSNL-1 efficiently sever actin filaments in a Ca^{2+}-dependent manner. In contrast, the gelsolin fragment containing the three N-terminal G domains severs actin filaments in a manner independent of calcium, but gelsolin fragments containing G1 or G1G2 have calcium-sensitive severing activity (*8*, *30*). Therefore, G3 of gelsolin masks the calcium sensitivity, but this is not the case for GSNL-1. Atomic structures of gelsolin show that G3 interacts with G1 in the absence of calcium and masks its actin binding site (*16*), but G3 is moved away from G1 when it binds to actin (*12*). Although intramolecular domain interactions in GSNL-1 are currently unknown, a mode of calcium-dependent conformational changes that involve G1 could be different between GSNL-1 and gelsolin.

G1G2 of GSNL-1 is the smallest fragment that has barbed end capping activity (Figure 9A and Table 1). G1a or G1b did not have capping activity, indicating that G2 is required for capping. In contrast, G1 and G2G3 of gelsolin can independently cap the barbed end (*9*, *31*). Since G1 of gelsolin has only one actin binding site, Weber et al. (*9*) predicted that binding of gelsolin G1 to the barbed end of F-actin induces a conformational change that will slow dissociation of the monomer from the end. Thus, G2 together with G1 of GSNL-1 may be required to cause such a change, or G2 may have an actin-binding site for a neighboring actin monomer at the barbed end, so that G1G2 can cross-link two monomers at the end to inhibit monomer dissociation. In either case, the difference in capping activity suggests that the actin−G1 interactions at the barbed end are somewhat different between GSNL-1 and gelsolin.

G1G2 of GSNL-1 is also the smallest fragment that binds to PIP2 (Figure 9A and Table 1). Interaction of G1a or G1b with PIP2 was only detected by weak PIP2 inhibition of actin fragmentation by pelleting assays, suggesting that G2 is important for PIP2 binding. In gelsolin, a PIP2 binding site is located in residues 135−169 that spans the C-terminus of G1 to the N-terminus of G2 (Figure 9B). This PIP2-binding site can be divided into two separate PIP2-binding sequences: P1 (residues 135−149) (*32*) and P2 (residues 150−169) (*33*). Comparison of the sequence of GSNL-1 and gelsolin shows that P2 is conserved in GSNL-1, but basic residues of gelsolin P1 are not conserved in GSNL-1. This suggests that the P2-like sequence in G2 of GSNL-1 is the primary PIP2-binding site. Since P2 of gelsolin is responsible for the PIP2 sensitivity (*34*), the P2-like sequence of GSNL-1 is predicted to be the PIP2 regulatory site.

The actin regulatory activities of GSNL-1 are expected to be adapted to its biological functions. Messenger RNA of GSNL-1 is enriched in striated muscle in *C. elegans* (*35*). However, our preliminary studies indicate that a null mutation of *gsnl-1* does not cause detectable changes in muscle actin organization under normal culture conditions (our unpublished data). Similarly, mammalian gelsolin is expressed in striated muscle and localizes to the thin filaments in myofibrils (*1*), but its role in muscle cells is not understood. Biochemical studies show that GSNL-1, as well as gelsolin, is regulated by calcium and PIP2, which are second messengers in a number of signaling pathways. Therefore, GSNL-1 might function in transient remodeling of the actin cytoskeleton upon signaling events during development and/or environmental stimuli. Our biochemical studies on GSNL-1 should provide basic knowledge to help further functional investigations of gelsolin-related proteins in *C. elegans* using genetic approaches.

REFERENCES

1. Ono, S. (2007) Mechanism of depolymerization and severing of actin filaments and its significance in cytoskeletal dynamics. *Int. Rev. Cytol. 258*, 1–82.
2. Sun, H. Q., Yamamoto, M., Mejillano, M., and Yin, H. L. (1999) Gelsolin, a multifunctional actin regulatory protein. *J. Biol. Chem. 274*, 33179–33182.
3. Silacci, P., Mazzolai, L., Gauci, C., Stergiopulos, N., Yin, H. L., and Hayoz, D. (2004) Gelsolin superfamily proteins: Key regulators of cellular functions. *Cell. Mol. Life Sci. 61*, 2614–2623.
4. McGough, A. M., Staiger, C. J., Min, J. K., and Simonetti, K. D. (2003) The gelsolin family of actin regulatory proteins: Modular structures, versatile functions. *FEBS Lett. 552*, 75–81.
5. Bamburg, J. R. (1999) Proteins of the ADF/cofilin family: Essential regulators of actin dynamics. *Annu. Rev. Cell Dev. Biol. 15*, 185–230.
6. Bamburg, J. R., McGough, A., and Ono, S. (1999) Putting a new twist on actin: ADF/cofilins modulate actin dynamics. *Trends Cell Biol. 9*, 364–370.
7. Ono, S. (2003) Regulation of actin filament dynamics by actin depolymerizing factor/cofilin and actin-interacting protein 1: New blades for twisted filaments. *Biochemistry 42*, 13363–13370.
8. Kwiatkowski, D. J., Janmey, P. A., and Yin, H. L. (1989) Identification of critical functional and regulatory domains in gelsolin. *J. Cell Biol. 108*, 1717–1726.
9. Weber, A., Pring, M., Lin, S. L., and Bryan, J. (1991) Role of the N- and C-terminal actin-binding domains of gelsolin in barbed filament end capping. *Biochemistry 30*, 9327–9334.
10. Pope, B., Way, M., and Weeds, A. G. (1991) Two of the three actin-binding domains of gelsolin bind to the same subdomain of actin. Implications of capping and severing mechanisms. *FEBS Lett. 280*, 70–74.
11. McLaughlin, P. J., Gooch, J. T., Mannherz, H. G., and Weeds, A. G. (1993) Structure of gelsolin segment 1-actin complex and the mechanism of filament severing. *Nature 364*, 685–692.
12. Burtnick, L. D., Urosev, D., Irobi, E., Narayan, K., and Robinson, R. C. (2004) Structure of the N-terminal half of gelsolin bound to actin: Roles in severing, apoptosis and FAF. *EMBO J. 23*, 2713–2722.
13. Robinson, R. C., Mejillano, M., Le, V. P., Burtnick, L. D., Yin, H. L., and Choe, S. (1999) Domain movement in gelsolin: A calcium-activated switch. *Science 286*, 1939–1942.
14. Van Troys, M., Dewitte, D., Goethals, M., Vandekerckhove, J., and Ampe, C. (1996) Evidence for an actin binding helix in gelsolin segment 2: Have homologous sequences in segments 1 and 2 of gelsolin evolved to divergent actin binding functions? *FEBS Lett. 397*, 191–196.
15. McGough, A., Chiu, W., and Way, M. (1998) Determination of the gelsolin binding site on F-actin: Implications for severing and capping. *Biophys. J. 74*, 764–772.
16. Burtnick, L. D., Koepf, E. K., Grimes, J., Jones, E. Y., Stuart, D. I., McLaughlin, P. J., and Robinson, R. C. (1997) The crystal structure of plasma gelsolin: Implications for actin severing, capping, and nucleation. *Cell 90*, 661–670.
17. Choe, H., Burtnick, L. D., Mejillano, M., Yin, H. L., Robinson, R. C., and Choe, S. (2002) The calcium activation of gelsolin: Insights from the 3A structure of the G4-G6/actin complex. *J. Mol. Biol. 324*, 691–702.

18. Klaavuniemi, T., Yamashiro, S., and Ono, S. (2008) *Caenorhabditis elegans* gelsolin-like protein 1 is a novel actin filament-severing protein with four gelsolin-like repeats. *J. Biol. Chem. 283*, 26071–26080.
19. Pardee, J. D., and Spudich, J. A. (1982) Purification of muscle actin. *Methods Enzymol. 85*, 164–181.
20. Kouyama, T., and Mihashi, K. (1981) Fluorimetry study of N-(1-pyrenyl)iodoacetamide-labelled F-actin. Local structural change of actin protomer both on polymerization and on binding of heavy meromyosin. *Eur. J. Biochem. 114*, 33–38.
21. Mohri, K., Vorobiev, S., Fedorov, A. A., Almo, S. C., and Ono, S. (2004) Identification of functional residues on *Caenorhabditis elegans* actin-interacting protein 1 (UNC-78) for disassembly of actin depolymerizing factor/cofilin-bound actin filaments. *J. Biol. Chem. 279*, 31697–31707.
22. Safer, D. (1989) An electrophoretic procedure for detecting proteins that bind actin monomers. *Anal. Biochem. 178*, 32–37.
23. Ono, S., McGough, A., Pope, B. J., Tolbert, V. T., Bui, A., Pohl, J., Benian, G. M., Gernert, K. M., and Weeds, A. G. (2001) The C-terminal tail of UNC-60B (ADF/cofilin) is critical for maintaining its stable association with F-actin and is implicated in the second actin-binding site. *J. Biol. Chem. 276*, 5952–5958.
24. Southwick, F. S. (1995) Gain-of-function mutations conferring actin-severing activity to human macrophage Cap G. *J. Biol. Chem. 270*, 45–48.
25. Zhang, Y., Vorobiev, S. M., Gibson, B. G., Hao, B., Sidhu, G. S., Mishra, V. S., Yarmola, E. G., Bubb, M. R., Almo, S. C., and Southwick, F. S. (2006) A CapG gain-of-function mutant reveals critical structural and functional determinants for actin filament severing. *EMBO J. 25*, 4458–4467.
26. Janmey, P. A., and Stossel, T. P. (1987) Modulation of gelsolin function by phosphatidylinositol 4,5-bisphosphate. *Nature 325*, 362–364.
27. Yin, H. L., Janmey, P. A., and Schleicher, M. (1990) Severin is a gelsolin prototype. *FEBS Lett. 264*, 78–80.
28. Janmey, P. A., and Matsudaira, P. T. (1988) Functional comparison of villin and gelsolin. Effects of Ca^{2+}, KCl, and polyphosphoinositides. *J. Biol. Chem. 263*, 16738–16743.
29. Irobi, E., Burtnick, L. D., Urosev, D., Narayan, K., and Robinson, R. C. (2003) From the first to the second domain of gelsolin: A common path on the surface of actin? *FEBS Lett. 552*, 86–90.
30. Chaponnier, C., Janmey, P. A., and Yin, H. L. (1986) The actin filament-severing domain of plasma gelsolin. *J. Cell Biol. 103*, 1473–1481.
31. Sun, H. Q., Wooten, D. C., Janmey, P. A., and Yin, H. L. (1994) The actin side-binding domain of gelsolin also caps actin filaments. Implications for actin filament severing. *J. Biol. Chem. 269*, 9473–9479.
32. Yu, F. X., Sun, H. Q., Janmey, P. A., and Yin, H. L. (1992) Identification of a polyphosphoinositide-binding sequence in an actin monomer-binding domain of gelsolin. *J. Biol. Chem. 267*, 14616–14621.
33. Janmey, P. A., Lamb, J., Allen, P. G., and Matsudaira, P. T. (1992) Phosphoinositide-binding peptides derived from the sequences of gelsolin and villin. *J. Biol. Chem. 267*, 11818–11823.
34. Xian, W., and Janmey, P. A. (2002) Dissecting the gelsolin-polyphosphoinositide interaction and engineering of a polyphosphoinositide-sensitive gelsolin C-terminal half protein. *J. Mol. Biol. 322*, 755–771.
35. Fox, R. M., Watson, J. D., Von Stetina, S. E., McDermott, J., Brodigan, T. M., Fukushige, T., Krause, M., and Miller, D. M. (2007) The embryonic muscle transcriptome of *Caenorhabditis elegans*. *Genome Biol. 8*, R188.
36. Feng, L., Mejillano, M., Yin, H. L., Chen, J., and Prestwich, G. D. (2001) Full-contact domain labeling: Identification of a novel phosphoinositide binding site on gelsolin that requires the complete protein. *Biochemistry 40*, 904–913.
37. Way, M., Pope, B., Gooch, J., Hawkins, M., and Weeds, A. G. (1990) Identification of a region in segment 1 of gelsolin critical for actin binding. *EMBO J. 9*, 4103–4109.
38. Pope, B., Maciver, S., and Weeds, A. (1995) Localization of the calcium-sensitive actin monomer binding site in gelsolin to segment 4 and identification of calcium binding sites. *Biochemistry 34*, 1583–1588.